The EuroBiotech Journal
RESEARCH ARTICLE
Bioengineering

A strategy for covalent anchoring of self-assembling β³ oligoamide nanorods to gold surfaces

Khadeeja A. Hussein[1], Ketav Kulkarni[2], Anders Barlow[1], Patrick Perlmutter[1], Adam Mechler[1*]

Abstract

Oligopeptides stand out for their remarkable structural variability, ease of synthesis, and amenability to functionalization, making them exceedingly appealing for crafting functional nanostructured materials. The low metabolic stability of natural peptides can be overcome by replacing α-amino acids with β³- amino acids, to yield artificial peptides best described as substituted β³-oligoamides. Controlling the morphology of such structures by varying the amino acid residues and altering the oligoamide termini makes it possible to adapt the core design to a range of hierarchical structures and function. Conductivity is a desired property in such nanomaterials; preferably conductive materials should be chemically anchored to a highly conductive metal, such as gold surface to connect to macroscopic electronics. It is preferable to use thiol functionality, however β³ cysteine is not synthetically achieveable. In this study β³ [SLIA] oligoamide has been synthesized and functionalized at the N terminus with a thiol moiety. After successful synthesis and purification, the thiolated oligoamide was physically characterized to confirm binding to gold, self-assembly and hetero assembly on these anchor points. It was demonstrated with a quartz crystal microbalance (QCM) that self-assembling monolayers can be formed on a gold surface and the formation of a S-Au bond was confirmed with X-ray photoelectron spectroscopy. Growth of Ac-β³[WKLWEL] fibres on these anchor points was confirmed by using atomic force microscopy and QCM. Hence, a viable metal anchor has been established that lays the foundations for the future development of molecular electronics based on β³ oligoamides.

Keywords: Substituted oligoamide, gold binding, self-assembly, hetero-assembly.

Introduction

Self-assembly is the spontaneous organization of molecules into complex structures that can be influenced by factors such as solvent, environment, temperature and pH[1]. It offers a design principle to create complex structures based on monomer units that are easy to produce and control, such as peptides [2-7]. Depending on the sequence, peptides can fold into different secondary structures, for example the α-helix or β-sheet [8-9]. These secondary structures may further assemble to form nanowires, nanotubes or nanofibrils that are considered for a wide range of applications such as biosensing and nanofabrication techniques[10]. However, α-peptides have inherent limitations including stimuli/sensitive folding, limited functionalizability without affecting structure, as well as limited chemical and metabolic stability that can lead to fast degradation [11-12]. Using unnatural β-amino acids, where an extra methylene group is present in the backbone of each unit in the oligoamide chain, offers the means to overcome limitations of α-peptides; for distinction these peptides can be called substituted oligoamides. The secondary structures of β-oligoamides are more diverse and thermodynamically stable, while also exhibiting higher metabolic and chemical stability[6-7, 13-18]. β-Oligoamides can fold into secondary structures to form sheets and a range of different types of helices[19]. These foldamers are defined by the physical properties of the amino acid residues such as stereochemistry, size,

[1] Department of Chemistry and Physics, La Trobe Institute for Molecular Science, La Trobe University, Bundoora, Victoria 3086, Australia
[2] Biomedicine Discovery Institute, Monash University, Clayton, VIC 3800, Australia

*** Corresponding Authors:**
Adam Mechler: a.mechler@latrobe.edu.au

DOI: 10.2478/ebtj-2024-0009

and the chemical properties of the sidechains[6, 15]. Helical structures include 14, 12, and 12/10/12 helices, where the designation indicates the number of atoms that make up one turn of the helix. These structures are stabilized by hydrogen bonding between amide NH protons and carbonyl oxygen in the backbone of the oligoamide chain. [9, 20-23]

For β^3-oligoamides the 14-helix fold is most stable. The 14-helix contains 3-3.1 residues per turn resulting in longitudinal alignment of the side chains along the helix that provides extra stability due to side chain interactions and a predictable structure for new materials with specific functionality[20-24]. We demonstrated that in β^3-oligoamides, intermolecular three-point hydrogen bonds can be easily formed by acetylation of terminal NH_2 group, yielding head to tail self-assembling helical nanorods using both intermolecular and intramolecular hydrogen bonding as we have demonstrated in a range of articles [1, 18, 22, 25-28]. We have shown that these stable nanorods further assemble in different solvent environments into either fibre bundles, mesh-like or dendritic structures[22, 25-29]. We have also demonstrated the co-assembly of Ac-β^3-oligoamides of different monomer units into structures that are analogous to co-polymers[28], offering extra flexibility in designing supramolecular structures and underpinning the work reported here.

A specific challenge towards designing self-assembling materials is to incorporate conductivity – based applications in e.g. molecular electronics or regenerative medicine [30-31]. In macromolecular systems, such as polymers, conductivity may be achieved by including conjugation or adding metal redox centers through coordination chemistry. It is challenging to transfer these principles to self-assembled materials; it is even more challenging to connect them to metal electrodes. Binding the conducting material to a metal surface is a key problem for molecular electronics[32]. It should be noted that immobilizing oligoamides or proteins to specific surfaces is also important to a wide range of other applications, in e.g. medicine, sensing and nanotechnology.[33] Chemical surface modifications are routinely used to bind polypeptides to a surface, typically in two-step process based on intermediate self-assembled monolayer (SAMs) of organic molecules on a metal.[33-34] SAMs on gold are typically reliant on thiol chemistry, and then oligopeptides are immobilized through routine coupling chemistry[35-38]. It is possible, however, to bind small oligoamides to surfaces using thiol chemistry without the need to involve a SAM.

In this paper we outline a solution for anchoring self-assembled β^3 oligoamide helices to gold surface by designing a synthetic strategy for thiolated versions of Ac-β^3 [SLIA] oligoamide that are known to self-assemble into helical superstructures. *N*-chlorinated β^3 [SLIA] oligoamide was synthesized and functionalized with a thiol moiety and characterized chemically using mass spectroscopy, ^{1}H-NMR and HPLC. Binding this oligoamide to gold was done as an anchor point for self-assembling N-acyl β^3 oligoamides. Hetero-assembly of *N*-acyl β^3[WKLWEL] on the anchor points was confirmed with microscopy and spectroscopy methods.

Materials and Methods

Solvents, including acetonitrile, were purchased from Sigma-Aldrich Pty. LTD. (Castle Hill, NSW, 2154 Australia). For some experiments, ultrapure water with a resistivity of 18.2 MΩ-cm was used (Sartorius AG, Germany).

1. Oligoamide synthesis and purification

Two β^3-oligoamides (Figure 1.: SH- β^3[SLIA] and Ac-

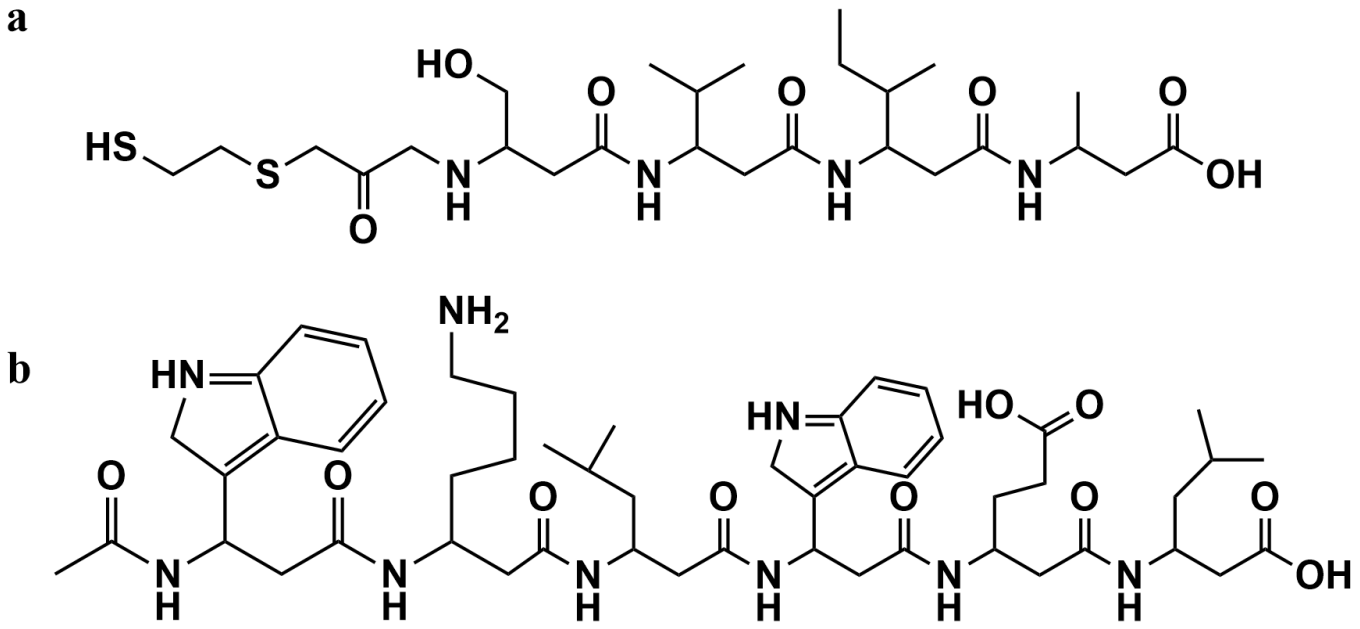

Figure 1. Chemical structures of (a) SH- β^3[SLIA] and (b) Ac- β^3[WKLWEL]

β³[WKLWEL]) were synthesized using solid phase oligoamide synthesis as reported previously[25]. In the case of the thiolated oligoamide, SH- β³[SLIA], *N*-terminus was acetylated by treating the oligoamide on resin with a solution of chloroacetic anhydride (171 mg), and 100 µL of DIPEA in 3 mL of DMF for 60 min. The capped resin was subsequently washed with DMF, DCM and Et_2O (2 × 5 min) and then air-dried for 10 min. The resin was treated with cleavage solution which consisted of 12 mL of TFA, an equal volume of water and 360 µL TIS by gentle rotation for 60 min. The crude was filtrated to remove the resin and the filtrate was concentrated with a stream of N_2 for TFA evaporation. The β-oligoamide solution was then diluted with 50% aqueous acetonitrile for lyophilisation. In order to functionalize the oligoamides, the cleaved β³-oligoamide was dissolved in 20 mL of 50% aqueous/acetonitrile along with NH_4HCO_3 (150 mg) and 100.65 µL of ethanedithiol and allowed to react for 48 hours. Reaction completion was confirmed by MS and the mixture was then lyophilized.

HPLC purification was conducted on a preparative HPLC system (1260 series Agilent Technologies) using a reverse-phase semi-preparative (Onyx Monolithic, C18, 10 mm x 100 mm) column (Phenomenex, Agilent Technologies) and detected at wavelengths of 220, 254 and 280 nm. The oligoamides were eluted over a 14 min gradient from 20 to 60 % solvent B, (solvent B: 0.1 % TFA/CH_3CN; solvent A: 0.1 % TFA/H_2O) with a flow rate of 7 mL/min. An analytical column was used to confirm purity. Mass and ^{1}H-NMR spectra for SH- β³[SLIA] synthesised oligoamides are included in the supporting information.

For the experiments, SH-β³[SLIA] solutions were prepared by dissolving 0.5 mg in 1ml of solvent mixture (3:8 acetonitrile:water – the minimum amount of acetonitrile to fully dissolve the material) and then centrifuged for 15 mins, while Ac-β³[WKLWEL] was prepared by dissolving 1 mg in 1 ml of ultra-pure water.

2. Surface binding experiments

2.1 Quartz crystal microbalance experiments

A Qsense QCM-D system (Qsense, Gothenburg, Sweden) was used with a single channel measurement unit. Given the sensitivity of the peristaltic pump tubing to organic solvents the pump module could not be used and thus an open QCM chamber system was used for all experiments. Measurements were performed at 20°C. The eigenfrequencies of a blank QCM sensor chip were measured first in 150 µl of 3:8 acetonitrile: water mixture and then followed by adding 50 µl of SH- β³[SLIA] solution for one hour. The frequency changes (difference between before and after modification) were used to monitor mass adsorption.

For co-assembly experiments the same thiolated QCM sensor was thoroughly washed to remove any unbound monomers and then the crystal was tuned in 100 µl of deionized water. The temperature was increased to 40°C and eigenfrequencies were monitored. After stabilizing the temperature and frequency, 50 µl of the Ac-β³[WKLWEL] solution was added, monitored for 4 hours and then left for 15 days at room temperature. Care was taken to ensure the solution did not evaporate. The eigenfrequency was measured every two days at 40°C to compare the mass changes. OriginPro software (OriginLab) was used to plot all QCM data.

2.2 X-ray photoelectron spectroscopy (XPS)

After depositing the thiolated peptides the QCM sensor was removed, washed and dried for XPS measurements. A Kratos Axis Nova spectrometer was used with Al Kα X-ray source (aluminium anode, pass energy of 20, dwell time 426 ms, sweeps of 25). The data were plotted using OriginPro software (OriginLab).

2.3 Sample preparations for AFM images

AFM imaging was conducted on samples deposited onto either freshly cleaved mica surface or QCM sensor. For mica substrates, 1 µl of two-months old, aged SH-β³[SLIA] solution was deposited on surface and imaged after drying. The ageing process is required to produce long one dimensional fibres, as the fibre growth is essentially one dimensional and it follows an Ostwald ripening pathway. Co-assembled oligoamide solution was prepared by mixing equal amount (30 µl) of SH- β³[SLIA] and Ac-β³[WKLWEL] in 60 µl of 3:8 acetonitrile: water mixture and aged for one week. 1 µl of this solution was deposited for imaging. QCM sensors were imaged after the completion of QCM experiments.

All samples were left to dry over two nights and an Ntegra AFM platform (NT-MDT, Russia) was used to image the samples with silicon probes of nominal 10 nm apex radius and typical spring constants of 1-15 Nm^{-1}. 87-230 kHz resonance frequency, 0.5 Hz scan rate with 512 × 512-pixel resolution. Gwyddion software (version 2.47) was used to process and analyse AFM images (http://gwyddion.net).

2.4 Experimental details of DLS measurements

50 µl of SH-β³[SLIA] solution in 3:8 acetonitrile: water mixture at 0.5 mg/ml concentration was measured in a plastic cuvette. Three repeat measurements were performed. The measurements were conducted using a Malvern Zetasizer Nano ZS instrument (Malvern Instruments Ltd., UK) at controlled temperatures. Number distribution plots were based on NNLS fit model. Three measurements were taken on each sample. DLS data was plotted using OriginPro software (OriginLab).

Results

The synthetic route to obtain oligoamide SH-β³[SLIA], is outlined in Figure 2. β³[SLIA] was synthesized on Wang resin and treated with chloroacetic anhydride on the resin. After cleavage from the resin, a thiol moiety was attached to the oligoamide by reaction with ethanedithiol. The oligoamide was purified successfully using HPLC and its structure confirmed by ^{1}H-NMR and mass spectrometry (see Supplementary data Figures S1,2 and 3).

To be able to use SH-β³[SLIA] as anchor points for attachment of other self-assembling oligoamides, it should be bound to

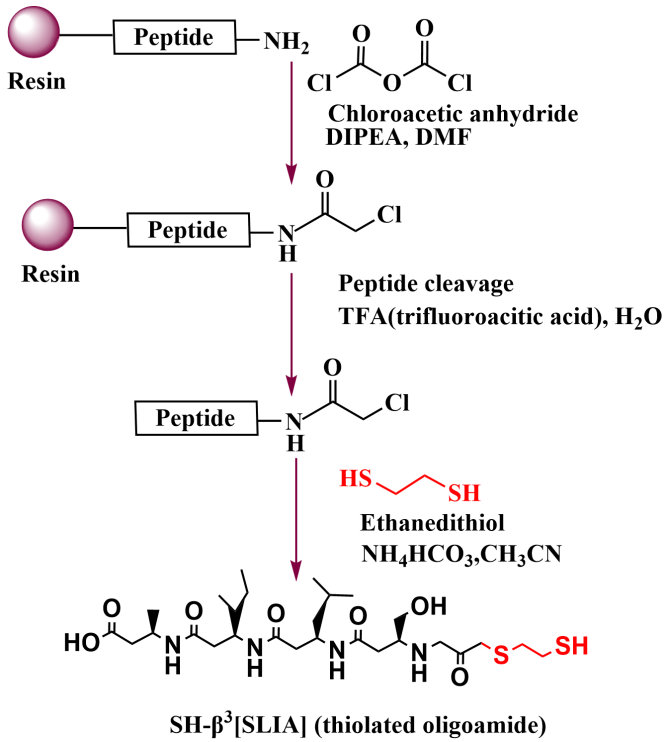

Figure 2. Functionalization of N-terminus for gold binding oligoamide

gold in monomeric form and so conditions were optimized for keeping SH-β³[SLIA] monomeric in solution. Dynamic light scattering was used to investigate the aggregation state of thiolated oligoamides in 3:8 acetonitrile:water mixture. At 20°C the results showed that SH-β³[SLIA] suspension is polydisperse but dominated by a population of a size less than

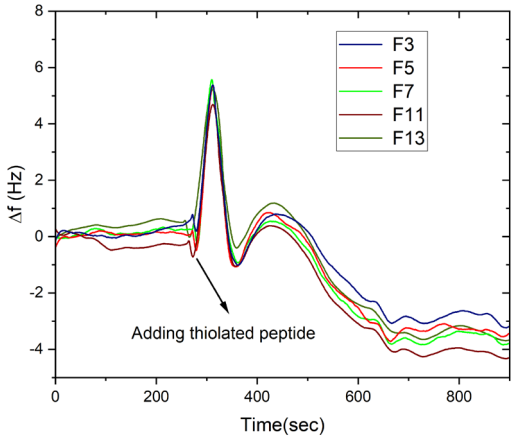

Figure 3. QCM frequency change of the binding of SH-β³[SLIA] to the gold surface the initial transient is due to injecting solution into the open cell.

1 nm as expected for monomer (see Supplementary data figure S4). Given the sensitivity of DLS to the 6th power of diameter this confirms that SH-β³[SLIA] is predominantly monomeric in acetonitrile-water solution at 0.5 mg/ml concentration.

This oligoamide can bind specifically to gold surface owing to -SH group. To confirm that the attachment takes place, QCM mass measurements were performed in real time in the same solvent mixture and temperature where monomer units dominate in the solution as confirmed by DLS. Figure 3 shows that, after an initial transient, the resonance frequency of the QCM sensor has decreased upon introducing the thiolated oligoamides. Decreasing frequency confirms increased mass, that is, binding of SH-β³ [SLIA] on the sensor chip surface. The -4 Hz frequency change is consistent with one sparse layer of SH-β³ [SLIA] on the QCM sensor; for comparison, a frequency change of around -6 Hz was reported before for the deposition of a tightly packed phospholipid monolayer on alkanethiol modified QCM sensor [39].

CM confirms attachment of SH-β³[SLIA] to the sensor surface but does not reveal whether it is physisorption or chemisorption. XPS can provide information about the binding energy of sulfur and the presence of S-Au bonds and so it was used to complement the QCM results. Figure

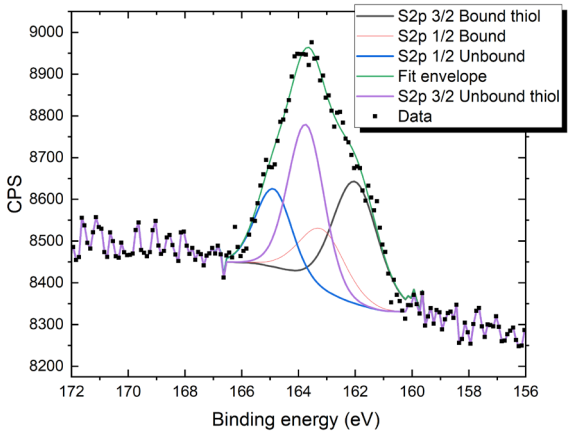

Figure 4. XPS spectra of S_{2p} of modified QCM surface with SH-β³ [SLIA] solution

4 shows the S_{2P} region of the XPS spectrum of the modified QCM surface. The characteristic intrinsic energy step of the XPS background was fitted in specialist software (Casa XPS) that was also used to fit the curve using known bond energies and shapes of S-H and S-Au peaks: the $S_{2p1/2}$ peak at binding energy of 165 eV, and the $S_{2p3/2}$ peak that has binding energy of 162 eV consistent with gold-bound sulfur[40-41]. Thus, QCM and XPS results provided evidence for chemisorption of thiolated oligoamides to the gold surface.

To grow nanorods on these anchor points, and to correctly characterize these as hetero-assembly it is critical to assess

the ability of SH-β³ [SLIA] to homo-assemble, which is to be avoided, and co-assemble with a reference oligoamide Ac-β³[WKLWEL] that is the desired outcome. AFM imaging was used to determine the changes in oligoamide morphology as evidence of homo-and co-assembly. AFM images of pure SH-β³[SLIA] show fibrous materials, hence the oligoamide can homo-assemble in spite of the terminal thiolation. The morphology of the thiolated peptide is dominated by thick layers of branching bundles of around 47 nm height (figure 5 A-B). AFM images in previous studies of Ac- β³[WKLWEL] in water showed large, fibrous bundle structures of very different appearance [42]. Mixing SH-β³ [SLIA] and Ac- β³[WKLWEL] yielded distinct, slightly dendritic structures (figure 5 C) with underlying parallel ribbon structure (figure 5 D) that is characteristically different from the fibres formed by the pure oligoamides, consistent with co-assembly into an organised arrangement that might also involve inter-fibril H-bonding of the thiol moiety. Thus, growing nanorods of a different oligoamide on the anchor points is feasible.

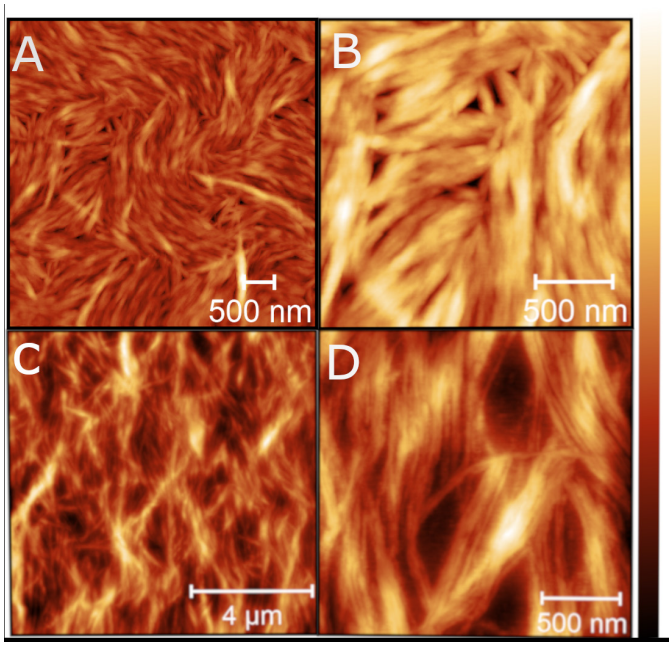

Figure 5. AFM images of self-assembled structures of the oligoamides SH-β³[SLIA] in its pure form (A, B) and co-assembled with Ac- β³[WKLWEL]. C and D All AFM images were recorded after two days of slow drying. Height is represented by colour scale (right of image) of (A) 47 nm, (B) 23 nm, (C) 65 nm and (D) 36 nm.

Nanorod growth on SH-β³ [SLIA] anchors

SH-β³[SLIA] deposited on gold QCM sensor was used as the anchoring point for Ac-β³[WKLWEL] nanorod growth in water**.** After binding SH-β³[SLIA] to the gold surface of QCM sensor and confirmed using QCM and XPS as per above, Ac-β³[WKLWEL] was introduced under condictions where it is mosly monomeric; this limits growth kinetics but allows for controlling the growth on the anchor sites without spontaneous fibre formation in the bulk of the solution. Optimizing the conditions suggests that Ac-β³[WKLWEL] is mostly monomeric at 40 °C, i.e. there is no non-specific aggregation, but there is scope for slow nanorod growth.. Hence, after an incubation time of 15 days at 40 °C, under continuous monitoring co-assembled nanorods of Ac-β³[WKLWEL] have grown on the anchoring thiolated oligoamide. As it can be seen from Figure 6, after four days of incubation the Δf decrease by 25-40 Hz and after 15 days it reduced by 45-60 Hz. Decreasing frequency of QCM sensor confirms the attachment of mass and thus the fibre formation of non-thiolated oligoamide on the anchoring

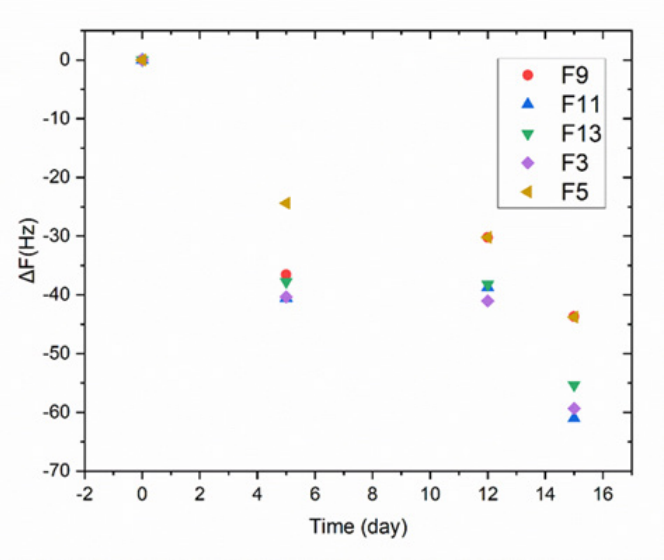

Figure 6. Frequency changes of co-assembly of Ac- β³ [WKL-WEL] to the anchoring point of SH- β³[SLIA] on gold surface: QCM frequency.

SH-β³[SLIA].

AFM imaging of nanorod growth

AFM for the three stages: bare gold surface, attachment of SH-β³[SLIA], and nanorod growth from this initial layer are shown in Figure 7. The morphology of the blank QCM sensor shows the gold nanoparticles with smooth surfaces and well-defined gaps between them (Figure 7A). These gaps narrow substantially and the top surface of the gold grains appears flatter after tyreatment with SH-β³ [SLIA] in 7B, without any appearance of grains or fibres. However, after nanorod growth, in figure 7C numerous grains/spikes appear on the surface the size and shape of which (figure 7 C) is defined by the convolution artefact of AFM imaging, id east, in case of

imaging very small structures the AFM tip shape is recorded on the image (Figure 7D). Thus, consistent with the QCM data, the AFM imaging suggests that the nanorods are sparse and only a few nanometres long. Significantly, they appear vertical, growing away from the surface.

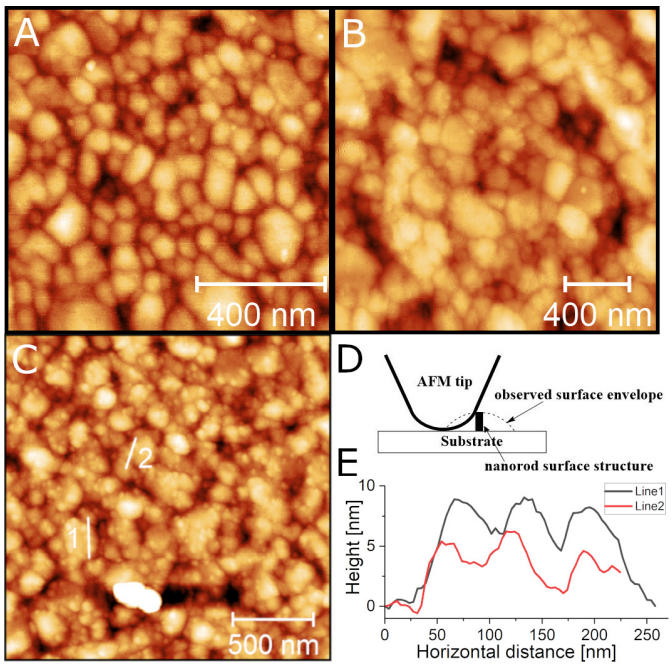

Figure 7. AFM images of QCM sensor. (A) images of blank QCM sensor (height scale 10 nm), (B) thiolated oligoamide attached, height of 36 nm; (C) is co-assembly of Ac-β³[WKLWEL] on SH-β³[SLIA] at height of 69 nm and (E) is the height profile for line 1 and 2 in (C); (D) is schematic diagram for the convolution in AFM images.

Discussion

The main aim of this study was to create anchor units of β³ oligoamides with thiol functionality for covalent attachment to gold electrode. For this, it is not possible to use cystein residues given that synthetic pathways for β³ amino acid analogue of cysteine have not been developed thus far. This necessitated the use of an alternative method. Importantly, there is no other strategy in existence to bind β³peptides to gold surface.

According to the experimental outcomes, successful synthesis and functionalisation of SH-β³[SLIA] was achieved through chlorinating the N-terminus and then thiolating using nucleophilic substitution, confirmed by H-NMR and mass spectroscopy. Binding of this oligoamide to a gold surface via S-Au bond was confirmed using XPS which showed a clear peak at 62 eV corresponding to the binding energy of the S-Au bond. Thus, the first aim, successful synthesis and covalent attachment of the anchor points to gold surface has been achieved.

The next aim was to grow nanorods of a different oligoamide on these anchor points, using the universal three point hydrogen bonding assembly motif described and characterized before[25, 43]. For this the oligoamide Ac- β³ [WKLWEL] was chosen, the self-assembling properties of which was thoroughly characterized before [28, 42] and so the focus was on hetero-attachment of these oligoamides on the established anchor points followed by homo-assembly to grow nanorods on the surface. The ability of Ac- β³ [WKLWEL] to hetero assemble with an oligoamide of the same self-assembly motif was shown before [28]. It was demonstrated with geometrical analysis that both oligoamides can homo-assemble under the right conditions, as well as co-assemble into a geometrically distinct superstructure. Hence, conditions had to be established where the thiolated peptide remains monomeric on the surface, that was confirmed with QCM mass measurement and AFM imaging, after which Ac-β³[WKLWEL] was introduced in monomeric form under conditions that substantially restrict the nanorod formation, to promote fibre growth from the surface but inhibit, as much as possible, self-assembly in solution. This was achieved by controlling the temperature and growing the nanorods over several days.

QCM confirmed the slow mass uptake and AFM images shows small vertical nanorods that appear round due to AFM tip deconvolution artefact, i. e. given the much smaller dimensions of the nanorod compared to the AFM tip, it is essentially the AFM tip that is imaged on the nanorod (figure 7C-H). Thus nanorods of Ac- β³oligoamides were successfully covalently anchored and grown on a gold substrate.

Conclusion

SH-β³[SLIA] oligoamide was synthesized and functionalized with a thiol moiety. After successfully purifying and chemically characterizing the oligoamide, QCM and AFM confirmed attachment to gold surface. The presence of S-Au bond was confirmed with X-ray photoelectron spectroscopy. Thus, "anchor" thiolated oligoamide for molecular electronic applications has been designed successfully. Hetero-assembly of N-acyl β³ [WKLWEL] on these anchor points was also successful. This metal anchor strategy forms the basis of molecular electronics applications based on co-assembled β³ oligoamides.

Conflict of interest

There are no conflicts to declare.

Acknowledgement

KH acknowledges La Trobe University, Australia, for PhD scholarship and Basra University for Oil and Gas, Iraq, for giving leave to study PhD.

References

1. Seoudi RS, Del Borgo MP, Kulkarni K, Perlmutter P, Aguilar M-I, Mechler A. Supramolecular self-assembly of 14-helical nanorods with tunable linear and dendritic hierarchical morphologies. New J. Chem. 2015; 39 (5): 3280-3287.
2. Mann S. Self-assembly and transformation of hybrid nano-objects and nanostructures under equilibrium and non-equilibrium conditions. Nat Mater 2009; 8 (10): 781-792.
3. Boyle AL, Bromley EH, Bartlett GJ, Sessions RB, Sharp TH, Williams CL, Curmi PM, Forde NR, Linke H, Woolfson DN. Squaring the circle in peptide assembly: from fibers to discrete nanostructures by de novo design. J Am Chem Soc 2012; 134 (37): 15457-15467.
4. Papapostolou D, Smith AM, Atkins ED, Oliver SJ, Ryadnov MG, Serpell LC, Woolfson DN. Engineering nanoscale order into a designed protein fiber. Proc Natl Acad Sci 2007; 104 (26): 10853-10858.
5. Ryadnov MG, Woolfson DN. MaP peptides: programming the self-assembly of peptide-based mesoscopic matrices. J Am Chem Soc 2005; 127 (35): 12407-12415.
6. Whitesides GM, Mathias JP, Seto CT Molecular self-assembly and nanochemistry: a chemical strategy for the synthesis of nanostructures; DTIC Document: 1991.
7. Whitesides GM, Grzybowski B. Self-assembly at all scales. Science 2002; 295 (5564): 2418-2421.
8. McMurry J. Organic Chemistry, Brooks. Cole, New York 1996: 657.
9. Seebach D, Hook DF, Glättli A. Helices and other secondary structures of β- and γ- peptides. J Pept Sci 2006; 84 (1): 23-37.
10. Yan X, Zhu P, Li J. Self-assembly and application of diphenylalanine-based nanostructures. Chem. Soc. Rev. 2010; 39 (6): 1877-1890.
11. Kemp DS. Construction and Analysis of Lifson Roig Models for the Helical Conformations of α-Peptides. Helv. Chim. Acta 2002; 85 (12): 4392-4423.
12. Werner HM, Horne WS. Folding and function in α/β-peptides: targets and therapeutic applications. Curr. Opin. Chem. Biol. 2015; 28: 75-82.
13. Hughes AB, Amino Acids, Peptides and Proteins in Organic Chemistry, Analysis and Function of Amino Acids and Peptides. John Wiley & Sons: 2013; Vol. 5.
14. Borenstein JT, Weinberg EJ, Orrick BK, Sundback C, Kaazempur-Mofrad MR, Vacanti JP. Microfabrication of three-dimensional engineered scaffolds. Tissue Eng. 2007; 13 (8): 1837-1844.
15. Gopalan RD, Del Borgo MP, Mechler AI, Perlmutter P, Aguilar M-I. Geometrically Precise Building Blocks: the Self-Assembly of β-Peptides. Chem Biol 2015; 22 (11): 1417-1423.
16. Uribe L, Gauss Jr, Diezemann G. Comparative Study of the Mechanical Unfolding Pathways of α-and β-Peptides. J Phys Chem B 2015; 119 (26): 8313-8320.
17. Beke T, Somlai C, Perczel A. Toward a rational design of β-peptide structures. J. Comput. Chem. 2006; 27 (1): 20-38.
18. Goodman CM, Choi S, Shandler S, DeGrado WF. Foldamers as versatile frameworks for the design and evolution of function. Nat Chem Biol 2007; 3 (5): 252-262.
19. Gellman SH. Foldamers: a manifesto. Acc. Chem. Res. 1998; 31 (4): 173-180.
20. DeGrado W, Schneider J, Hamuro Y. The twists and turns of β-peptides. J. Pept. Res. 1999; 54 (3): 206-217.
21. Craig CJ, Goodman JL, Schepartz A. Enhancing β3-Peptide Bundle Stability by Design. ChemBioChem 2011; 12 (7): 1035-1038.
22. Seoudi RS, Hinds MG, Wilson DJ, Adda CG, Del Borgo M, Aguilar M-I, Perlmutter P, Mechler A. Self-assembled nanomaterials based on beta (β 3) tetrapeptides. J Nanotechnol 2016; 27 (13): 135606.
23. Appella DH, Christianson LA, Klein DA, Powell DR, Huang X, Barchi Jr JJ, Gellman SH. Residue-based control of helix shape in beta-peptide oligomers. Nature 1997; 387 (6631): 381.
24. Cheng RP, Gellman SH, DeGrado WF. β-Peptides: from structure to function. Chem. Rev. 2001; 101 (10): 3219-3232.
25. Del Borgo MP, Mechler AI, Traore D, Forsyth C, Wilce JA, Wilce MC, Aguilar MI, Perlmutter P. Supramolecular Self-Assembly of N-Acetyl-Capped β-Peptides Leads to Nano- to Macroscale Fiber Formation. Angew. Chem. Int. Ed. 2013; 52 (32): 8266-8270.
26. Seoudi RS, Dowd A, Smith BJ, Mechler A. Structural analysis of bioinspired nano materials with synchrotron far IR spectroscopy. PCCP 2016; 18 (16): 11467-11473.
27. Seoudi RS, Dowd A, Del Borgo M, Kulkarni K, Perlmutter P, Aguilar M-I, Mechler A. Amino acid sequence controls the self-assembled superstructure morphology of N-acetylated tri-β3-peptides. Pure Appl. Chem. 2015; 87 (9-10): 1021-1028.
28. Buchanan C, Garvey CJ, Perlmutter P, Mechler A. Co-assembly of helical β3-peptides: a self-assembled analogue of a statistical copolymer. Pure Appl. Chem. 2017; 89 (12): 1809-1816.
29. Del Borgo MP. Supramolecular self-assembly of 14-helical nanorods with tunable linear and dendritic hierarchical morphologies. New J. Chem. 2015; 39 (5): 3280-3287.
30. Balint R, Cassidy NJ, Cartmell SH. Conductive polymers: towards a smart biomaterial for tissue engineering. Acta biomaterialia 2014; 10 (6): 2341-2353.
31. Rama G, Ardá A, Maréchal JD, Gamba I, Ishida H, Jiménez-Barbero J, Vázquez ME, Vázquez López M. Stereoselective formation of chiral metallopeptides. Chem Eur J 2012; 18 (23): 7030-7035.
32. Draxl C, Nabok D, Hannewald K. Organic/inorganic hybrid materials: Challenges for ab initio methodology. Acc. Chem. Res. 2014; 47 (11): 3225-3232.
33. Kühnle A. Self-assembly of organic molecules at metal

surfaces. Curr opin 2009; 14 (2): 157-168.
34. Kawasaki M, Sato T, Tanaka T, Takao K. Rapid self-assembly of alkanethiol monolayers on sputter-grown Au (111). Langmuir 2000; 16 (4): 1719-1728.
35. Cui Y, Kim SN, Naik RR, McAlpine MC. Biomimetic peptide nanosensors. Acc. Chem. Res. 2012; 45 (5): 696-704.
36. Sharif AM, Laffir FR, Buckley DN, Silien C. Distinct self-assembly of dithiol monolayers on Au (111) in water and hexane. Chem. Phys. 2014; 441: 77-82.
37. Hamoudi H, Guo Z, Prato M, Dablemont C, Zheng WQ, Bourguignon B, Canepa M, Esaulov VA. On the self assembly of short chain alkanedithiols. PCCP 2008; 10 (45): 6836-6841.
38. Qu D, Kim B-C, Lee C-WJ, Ito M, Noguchi H, Uosaki K. 1, 6-Hexanedithiol self-assembled monolayers on Au (111) investigated by electrochemical, spectroscopic, and molecular mechanics methods. J Phys Chem C 2009; 114 (1): 497-505.
39. Zhi Z, Hasan IY, Mechler A. Formation of alkanethiol supported hybrid membranes revisited. Biotechnol J 2018; 13 (12): 1800101.
40. Nuzzo RG, Zegarski BR, Dubois LH. Fundamental studies of the chemisorption of organosulfur compounds on gold (111). Implications for molecular self-assembly on gold surfaces. J Am Chem Soc 1987; 109 (3): 733-740.
41. Bourg M-C, Badia A, Lennox RB. Gold– sulfur bonding in 2D and 3D self-assembled monolayers: XPS characterization. The Journal of Physical Chemistry B 2000; 104 (28): 6562-6567.
42. Buchanan C, Garvey CJ, Puskar L, Perlmutter P, Mechler A. Coordination crosslinking of helical substituted oligoamide nanorods with Cu (II). Supramol. Chem. 2020; 32 (3): 222-232.
43. Buchanan C, Hinds MG, Puskar L, Garvey CJ, Mechler A. Comprehensive multidimensional study of the self-assembly properties of a three residue substituted β3 oligoamide. Pure Appl. Chem. 2021; 93 (11): 1327-1341.